

9-1-2018

## Selective bladder denervation for overactive bladder (OAB) syndrome: From concept to healing outcomes using the ovine model

James Fugett II  
*West Virginia University*

Lynette Phillips  
*American Preclinical Services*

Emily Tobin  
*American Preclinical Services*

Eric Whitbrook  
*Amphora Medical, Inc.*

Haydon Bennett  
*West Virginia University*

*See next page for additional authors*

Follow this and additional works at: <https://researchrepository.wvu.edu/ctsi>



Part of the [Medicine and Health Sciences Commons](#)

---

### Digital Commons Citation

Fugett, James II; Phillips, Lynette; Tobin, Emily; Whitbrook, Eric; Bennett, Haydon; Shrouf, Joshua; and Coad, James E., "Selective bladder denervation for overactive bladder (OAB) syndrome: From concept to healing outcomes using the ovine model" (2018). *Clinical and Translational Science Institute*. 954.  
<https://researchrepository.wvu.edu/ctsi/954>

This Article is brought to you for free and open access by the Centers at The Research Repository @ WVU. It has been accepted for inclusion in Clinical and Translational Science Institute by an authorized administrator of The Research Repository @ WVU. For more information, please contact [ian.harmon@mail.wvu.edu](mailto:ian.harmon@mail.wvu.edu).

---

**Authors**

James Fugett II, Lynette Phillips, Emily Tobin, Eric Whitbrook, Haydon Bennett, Joshua Shrout, and James E. Coad



# HHS Public Access

Author manuscript

*NeuroUrol Urodyn.* Author manuscript; available in PMC 2019 September 01.

Published in final edited form as:

*NeuroUrol Urodyn.* 2018 September ; 37(7): 2097–2105. doi:10.1002/nau.23560.

## Selective bladder denervation for overactive bladder (OAB) syndrome: From concept to healing outcomes using the ovine model

James Fugett II, BS<sup>1</sup>, Lynette Phillips, DVM<sup>2</sup>, Emily Tobin, BS<sup>2</sup>, Eric Whitbrook, BS<sup>3</sup>, Haydon Bennett, BS<sup>1</sup>, Joshua Shrout<sup>1</sup>, and James E. Coad, MD<sup>1</sup>

<sup>1</sup>Pathology Laboratory for Translational Medicine, West Virginia University School of Medicine, Morgantown, West Virginia

<sup>2</sup>American Preclinical Services, Minneapolis, Minnesota

<sup>3</sup>Amphora Medical, Inc., Maple Grove, Minnesota

### Abstract

**Aims:** We evaluated a Selective Bladder Denervation (SBD) device, which uses radiofrequency ablation, for the treatment of overactive bladder syndrome in terms of its nerve denervation, ablation characteristics, and post-treatment healing.

**Methods:** Using the SBD device, eight fresh extirpated ovine bladder trigones were treated (90°C set point for 60 s) and nitroblue tetrazolium viability stained to characterize the ablation. In addition, 12 trigones were treated in vivo with three adjacent ablations and divided into survival cohorts: Day 7, Day 30, and Day 90 to assess the ablations and their associated healing.

**Results:** The ex vivo single trigone ablations had a  $7.9 \pm 0.9$  mm width and  $5.7 \pm 1.0$  mm thickness that involved the submucosa, detrusor muscle, adventitia, and vagina. Microscopic viability staining confirmed complete nerve necrosis within the targeted tissue. The in vivo Day 7 trigones supported the ex vivo ablation characteristics and showed up to minimal inflammation, granulation tissue, and collagen fibrosis. Day 30 trigones had essentially absent inflammation and granulation tissue with evolving collagen fibrosis at the ablation's periphery. Day 90 trigones had essentially absent acute inflammation, minimal chronic inflammation, essentially absent granulation tissue, and up to mild collagen fibrosis. No ureteral/urethral alterations, vesico-vaginal fistulas, or other complications were identified.

**Conclusions:** The SBD device provided a targeted trigone ablation with resultant denervation. The tissue healing timeline followed that expected for a hyperthermic ablation and was

---

This is an open access article under the terms of the Creative Commons Attribution-NonCommercial License, which permits use, distribution and reproduction in any medium, provided the original work is properly cited and is not used for commercial purposes. <http://creativecommons.org/licenses/by-nc/4.0/>

**Correspondence** James E. Coad, MD, Pathology Laboratory for Translational Medicine, West Virginia University Department of Pathology, HSC-North, Mailstop 9203, 1 Medical Center Drive, 26506 Morgantown, WV., [jcoad@hsc.wvu.edu](mailto:jcoad@hsc.wvu.edu).

Performing Laboratories: (1) Pathology Laboratory for Translational Medicine, West Virginia University School of Medicine, Morgantown, WV 26506.

(2) American Preclinical Services, LLC 8945 Evergreen Blvd., Minneapolis, MN 55433.

characterized by a fibroproliferative healing response with limited inflammation and granulation tissue. The ablations did not impact the overlying bladder mucosal surface.

### Keywords

denervation; overactive bladder; tissue ablation; tissue healing

## 1 | INTRODUCTION

Overactive Bladder (OAB) is a condition that affects approximately 17% of women in the United States.<sup>1</sup> It is characterized by urinary urgency that may have associated urge incontinence, increased frequency, and/or nocturia.<sup>2</sup> Physiologically, micturition is achieved by parasympathetic stimulation of the detrusor muscle with simultaneous relaxation of the bladder outlet.<sup>3</sup> More specifically, the pelvic nerves stimulate muscarinic acetylcholine receptors within the bladder's trigone that initiate detrusor muscle contraction and subsequent urination.

While the pathophysiologic mechanism(s) of OAB have not been definitively ascertained, investigators have proposed both neurogenic and myogenic etiologies. The neurogenic etiology postulates that afferent innervation of the urothelial mucosa and submucosa provides altered luminal sensing that leads to urgency and unstable detrusor contractions.<sup>4,5</sup> Afferent nerves in the bladder are predominantly made of two fiber types: A $\delta$  and C-fibers. A $\delta$  fibers are thought to transmit stretch signals from throughout the bladder while C-fibers predominantly transmit signals related to bladder irritation and are located predominantly within the base of the bladder.<sup>6</sup> It is not known what role, if any, C-fibers play in normal micturition; but, they are up-regulated in hypersensitive bladder conditions such as cystitis, neurogenic bladder, and OAB. Teleological arguments have been proposed that suggest the role of C-fibers is to detect noxious/chemical stimuli or infections in the bladder. There is increasing evidence that the symptoms of OAB are caused by these afferent C-fiber type nerves that are densely located below the trigone. Thus, the trigone has been the focus of several studies on C-fiber activation and bladder hypersensitivity.<sup>7</sup>

Stemming from this proposed mechanism, a number of therapeutic approaches to alleviate OAB symptoms have emerged, including systemic pharmacological muscarinic receptor inhibition, adrenergic stimulation, intravesical OnabotulinumtoxinA injections, and the Modified Ingelman-Sundberg (MIS) surgical denervation procedure. As muscarinic receptors are expressed in several different tissues (including salivary glands and intestines), systemic muscarinic antagonists do not exclusively target the bladder with resultant possible clinical side effects unrelated to the patient's OAB.<sup>8,9</sup> Similarly, adrenergic receptors are also located throughout the body with resultant side effects, especially important being cardiovascular effects.<sup>10</sup> While more targeted than the systemic approach with potentially fewer side effects, OnabotulinumtoxinA injections provide a minimally invasive treatment that needs to be repeated to maintain clinical efficacy.<sup>11</sup> While potentially more durable, the MIS procedure involves an invasive surgery with more tissue disruption, longer recovery time, and potential for inter-procedural variations.<sup>12,13</sup> Therefore, an OAB therapy that

combines a minimally invasive targeted approach with clinical durability would improve therapeutic options for these patients.

A minimally invasive Selective Bladder Denervation (SBD) device (Amphora Medical, Maple Grove, MN) has been designed for the treatment of OAB (Figure 1A). The system includes a disposable transurethral device that accepts a rigid endoscope for visualization and has a lumen to facilitate addition and removal of fluids in the bladder. At the end of the lumen is a suction paddle to allow stabilization of the tissue and facilitate delivery of the RF electrodes powered by a suitable RF generator. The SBD device has been designed to provide a bipolar RF trigone-targeted ablation that denervates the underlying nerves that is followed by a type 1 collagen fibroproliferative healing response. As the clinical outcome is dependent on both the tissue's primary thermal ablation and healing response, the purpose of this study was to determine the SBD device's ablation characteristics and assess its resultant healing response using the Day 0 (extirpated) and in vivo Day 7, Day 30, and Day 90 ovine bladder model.

## 2 | MATERIALS AND METHODS

### 2.1 | Ex vivo bladder preparation, treatment, and evaluation

Fresh non-frozen extirpated ovine bladders, with preservation of the surrounding tissues including the vagina, were received from a local abattoir within 2 h of the ovine's euthanasia. The bladders were ventrally opened via a midline sagittal incision from the bladder neck to dome (Figure 1B). The bladders were pinned for stabilization, secured in a thin walled plastic bag with a saline gauze for humidification, and brought to  $37 \pm 1^\circ\text{C}$  in a saline bath just prior to ablation. After removing the plastic bag, the SBD device was positioned over the trigone in the saline bath, stabilized using the mucosal suction paddle, and then two RF electrodes were inserted into the underlying bladder wall. The bladders were treated with the SBD device powered by a RF generator (Neurotherm NT 2000iX, Abbott Laboratories, Abbott Park, IL), using Lesion Mode to maintain a  $90^\circ\text{C}$  temperature set point for 60 s based on prior developmental studies performed to identify the treatment parameters needed to create the optimal ablation described in this study.

The post-ablated bladders were maintained for approximately 3 h at room temperature after the ablation, rapidly frozen to  $-80^\circ\text{C}$ , transversely sectioned based on the suction paddle location, embedded on OCT cryomolds, frozen sectioned at 10 microns, nitro blue tetrazolium (NBT)-stained (Figure 1C) and evaluated using routine light microscopy. Tissue controls were also prepared, NBT-stained, and evaluated from the adjacent non-treated trigone region to ensure preservation of tissue quality and viability during the procedure. The NBT cytochemical viability stain utilizes intracellular dehydrogenase enzyme (*diaphorases*) with its cofactor (NADH/NADPH) to convert the colorless tetrazolium salt into a blue/violet formazan pigment in tissues with preserved enzymatic activity (NBT-positive, viable tissue). Ablated tissues, in which this enzymatic pathway is unable to metabolize the tetrazolium, do not stain and remain their native color (yellow-tan, NBT-negative, non-viable tissue).

## 2.2 | In vivo bladder treatment, necropsy, tissue preparation, and evaluation

The in vivo testing was performed at American Preclinical Services (APS, Minneapolis, MN) a licensed test facility with the United States Department of Agriculture to conduct research in laboratory animals. This study was reviewed and approved by the APS Institutional Animal Care and Use Committee (IACUC) prior to study initiation and was performed in accordance with Good Laboratory Practices (GLP). Each animal was prepped, brought to the procedure room, catheterize to drain the bladder, and then the bladder was filled with sterile saline until the urothelial bladder wall folds were visually removed. The in vivo treatments consisted of three adjacent ablations with the same parameters as the ex vivo ablations (Lesion Mode to maintain a 90°C temperature set point for 60 s). After visually localizing the suction paddle within the trigone and inserting the two electrodes into the bladder wall, radiofrequency energy was used to ablate the targeted bladder wall and associated nerves. The animals were then survived for  $7 \pm 1$ ,  $30 \pm 2$ , or  $90 \pm 2$  days prior to euthanasia.

Following euthanasia, an abdominal and pelvic necropsy was performed. Upon opening the abdominal cavity, the bowel, urinary bladder, ureters, kidneys, uterus, cervix, vagina, rectum, urethra, and other abdominal/pelvic structures were inspected in situ for any macroscopic signs of thermal injury and/or lesions. The distal ureters, urinary bladder, urethra, uterus, fallopian tubes, ovaries, cervix, vagina, rectum, and surrounding tissues were then dissected en bloc and fixed in 10% neutral buffered formalin. The urinary bladder, including the trigone and ureteral ostia, was transversely sectioned (approximately 5-8 mm intervals) from the proximal urethra across the bladder neck to the bladder apex. The trigone region, to encompass both the ablation and ureteral ostia, was submitted for routine formalin fixation, paraffin embedding, and both hematoxylin and eosin and trichrome staining on 5-micron tissue sections.

## 2.3 | Microscopic evaluation

The slides were histologically evaluated to characterize the ablations, including the involved tissue layers (epithelium, submucosa, detrusor muscle, adventitia, and/or deeper tissue extension). The residual ablation size was measured using a calibrated ocular micrometer to within  $\pm 0.1$  mm. In addition, the ablation-associated tissue healing reactions were scored for acute inflammation, chronic inflammation, granulation tissue, fibrosis, and overall healing stage (Table 1). In brief, polymorphonuclear leukocyte inflammation was defined as the presence of PMN-neutrophils at or associated with the ablation site. Chronic inflammation was defined as the presence of lymphocytes, histiocytes (monocyte-derived cells) and/or plasma cells associated with the ablation site. Granulation tissue was defined as the presence of new capillary angiogenesis in a loose connective tissue background associated with the ablation site. Fibrosis was defined as the presence of fibrocollagenous tissue healing, as a result of a wound-type healing reaction at the ablation site. The overall stage of healing was scored as essentially absent, loose early (granulation tissue with inflammation), primary healing (collagen deposition), or secondary healed scar.

## 3 | RESULTS

### 3.1 | Ex vivo bladder treatments

The eight ex vivo trigone single ablations had a mean NBT-negative width of  $7.9 \pm 0.9$  mm and thickness of  $5.7 \pm 1.0$  mm. These ablations were performed without difficulty. The NBT-stained sections demonstrated that each of the ablations ( $n = 8$ ) involved the underlying submucosa, detrusor muscle, adventitia, and adjacent vaginal wall tissues (Figures 1C and 2A). The adjacent non-treated trigone tissue from the bladders histologically confirmed the preservation of intact viable tissue without any alterations in NBT staining, thermal tissue changes, or tissue degradation.

### 3.2 | In vivo bladder treatments ( $n = 4$ ) – day 7 microscopic evaluation (Figure 2B)

No procedural or post-procedural treatment-related complications were identified during the in life post-treatment follow-up period and necropsies. All of the Day 7 trigone ablations involved the submucosa, detrusor muscle, adventitia, and vagina (100%). The three adjacent ablations approximated  $16.3 \pm 1.2$  mm (median: 16.3 mm) in width and  $8.4 \pm 1.6$  mm (median: 8.5 mm) in height (Table 2). The ablations were all histologically characterized by thermal tissue necrosis (coagulative necrosis with pale ghost-like tissue staining) with essentially absent (25%), minimal (50%) to mild (25%) acute inflammation (scaled score:  $0.8 \pm 0.8$ , median 0.5), essentially absent (50%) to minimal (50%) chronic inflammation (scaled score:  $0.5 \pm 0.5$ , median 0.5), patchy minimal (75%) to mild (25%) granulation tissue (scaled score:  $1.3 \pm 0.4$ , median 1.0), and essentially absent collagen fibrosis (scaled score:  $0.0 \pm 0.00$ , median 0) at the ablation's edge, consistent with the early phase of tissue healing.

### 3.3 | In vivo bladder treatments ( $n = 4$ ) – day 30 microscopic evaluation (Figure 2C)

No procedural or post-procedural treatment-related complications were identified during the in life post-treatment follow-up period and necropsies. The Day 30 trigone ablations involved the urothelium (25%), submucosa (25%), detrusor muscle (100%), adventitia (100%), and/or outer vaginal wall (75%). The healing ablation sites approximated  $13.9 \pm 2.8$  mm (median: 14.0 mm) in width and  $2.6 \pm 0.9$  mm (median: 2.3 mm) in height (Table 2). The ablations were characterized by essentially absent (75%) to moderate (25%) acute inflammation (scaled score:  $0.8 \pm 1.3$ , median 0), minimal (50%) to moderate (50%) chronic inflammation (scaled score:  $2.0 \pm 1.0$ , median 2.0), essentially absent (75%) to mild (25%) granulation tissue (scaled score:  $1.0 \pm 0.7$ , median 1.0), and a minimal (25%) to mild (75%) increase in collagen fibrosis (scaled score:  $1.8 \pm 0.4$ , median 2.0), consistent with primary phase of tissue healing.

### 3.4 | In vivo bladder treatments ( $n = 4$ ) – day 90 microscopic evaluation (Figure 2D)

No procedural or post-procedural treatment-related complications were identified during the in life post-treatment follow-up period and necropsies. The Day 90 ablated trigone regions involved the detrusor muscle (100%), adjacent adventitia (100%), and approximated  $13.1 \pm 4.5$  mm (median: 13.1 mm) in width and  $1.3 \pm 0.3$  mm (median: 1.3 mm) in height (Table 2). The ablation sites were characterized by essentially absent acute inflammation (100%,

scaled score:  $0.0 \pm 0.00$ , median 0), minimal (25%), mild (50%) to extensive (25%) chronic inflammation (scaled score:  $2.3 \pm 1.1$ , median 2.0), essentially absent granulation tissue (100%, scaled score:  $0.0 \pm 0.00$ , median 0), and a moderate increase in collagen fibrosis (scaled score:  $3.0 \pm 0.00$ , median 3.0), consistent with the secondary phase of tissue healing.

## 4 | DISCUSSION

Normal micturition is the result of voluntarily initiated parasympathetic stimulation of the detrusor muscle resulting in contraction of the detrusor. It is thought that up-regulation of sensory afferent nerves, in the bladder's trigone and base, result in the sensation of urgency at small bladder volumes.<sup>14,15</sup> This then causes an involuntary contraction of the detrusor via a spinal reflex and leads to urgency incontinence. Past investigators have proposed the modified Ingelman-Sundberg (MIS) procedure as a treatment for OAB. This surgical procedure involves an anterior vaginal wall incision followed by a sharp dissection to separate the vaginal wall from the bladder. This effectively resulted in denervation of the afferent supply to the bladder base and trigone. A patient's potential response to sub-trigonal denervation can be pre-operatively assessed using local anesthetics, such as bupivacaine, injected into this region.<sup>13</sup> Patients who demonstrated a reduction in symptoms and subsequently underwent a MIS procedure showed a partial to complete long-term response following surgery in 68% of cases.<sup>13</sup> More recently, OAB has been treated with less invasive approaches, including OnabotulinumtoxinA injection, with shorter periods of symptomatic relief necessitating retreatment. Therefore, an OAB therapy that combines a minimally invasive targeted approach with clinical durability would improve therapeutic options for these patients.

The SBD device (Amphora Medical) provides targeted bipolar radiofrequency trigone ablation to thermally denervate the underlying sensory nerves, which is then followed by a type 1 collagen fibroproliferative healing response. The SBD device emulates the MIS procedure in that they both denervate the trigone with a subsequent type 1 fibroproliferative healing response that may serve as a potential barrier to re-innervation; however, the SBD device does such in a significantly less invasive fashion.

The MIS procedure is technically challenging and inadvertent entry into the bladder lumen can occur. In contrast, the SBD device is minimally invasive. It utilizes cystoscopic guidance through the urethra to the trigone where two bipolar radiofrequency electrodes are inserted to ablate the nerves that course through the region between the bladder and vaginal walls. Various routes to access this targeted ablation region were considered. The transurethral route was selected given its minimally invasive nature and the ability to directly visualize treatment landmarks (ureteral ostia and bladder neck), more standardized distance between the urothelium and underlying target tissue than perineal or vaginal approaches and a more sterile approach than the clean-contaminated nature of a vaginal operative field. In addition to radiofrequency energy, other thermotherapy modalities may have the potential to similarly achieve similar trigonal denervation.

Given its similarities with the human urinary bladder wall thickness, the ovine bladder model was utilized to assess the SBD Device's resultant tissue effects. Although human

bladders are similar in volume to canine and swine, these models have thinner bladder walls. As this study was focused on the bladder wall's treatment effects, it was preferable to use the ovine model with a more similar wall thickness rather than overall size and shape.<sup>16</sup> As this treatment will initially be studied in women, the female ovine model was chosen to evaluate this device in the most representative anatomy, which included the vaginal wall and overlying bladder trigone.

With regards to correlations with the human bladder, ultrasonography of the trigone region's bladder wall thickness was  $5.8 \pm 0.1$  mm based on the study of 492 female patients.<sup>17</sup> In a separate study, patients with OAB were shown to have a greater bladder wall thickness compared to non-OAB patients ( $4.3 \pm 1.21$  mm and  $3.3 \pm 1.01$  mm, respectively).<sup>18</sup> Based on the evaluation of 14 female cadavers, Amphora Medical (unreported data) found the adventitial thickness, between the bladder wall and vagina, to be approximately 1 mm. The underlying anterior vaginal wall thickness has been reported to be  $2.7 \pm 0.6$  mm.<sup>19</sup>

Using the ex vivo fresh ovine bladder model, the SBD device demonstrated its ability to target the underlying trigonal nerves within the submucosa, detrusor muscle, and adventitia. Within these ablations, NBT viability staining confirmed complete necrosis of the nerves within and passing through the sub-trigone region, which would result in the interruption of afferent and efferent nerve signaling below the urothelium (Figures 3A and 3B). Subsequently, the in vivo ablations had similar tissue ablation characteristics (Figures 3C and 3D). At Day 7, the ablations were characterized by thermal tissue necrosis with minimal associated tissue healing. At 30 days there was variable residual thermal tissue necrosis, minimal inflammation, and early collagen deposition that began to replace the local tissues, consistent with the primary stage of healing. At Day 90, no residual thermal tissue necrosis remained with complete replacement by mature type 1 collagen, consistent with the secondary stage of healing. This fibrosis layer showed linearized compacted collagen fibrils that formed a dense tissue mat that connected with the detrusor muscle on either side of the ablation. This latter layer of collagen rich fibrosis histologically replaced the nerves and tissues that originally comprised this region and should provide a barrier to resist re-innervation of and through the ablated region. Future studies with longer follow-up will be necessary to fully assess the potential for trigonal re-innervation following the SBD procedure. Overall, the healing timeline in this study is within that expected for a focused/localized hyperthermic ablation.

This minimally invasive device was designed to mitigate the risk of potential for side effects, including unintended adjacent tissue injury (ureteral ostia, bladder neck, and adjacent organs), urinary retention, and vesico-vaginal fistula formation. The direct visualization of the ureteral ostia and bladder neck in combination with a suction paddle to stabilize the tissue during the ablation protect these adjacent structures. While indiscriminate nerve ablation within bladder could lead to bladder dysfunction, urinary retention, or worsening OAB and inadvertent bladder neck ablation could lead to worsening stress urinary incontinence (SUI), the Amphora OAB System specifically limits denervation to the sub-trigone region, while leaving the remainder of the bladder body and neck untreated. The intent of this is to denervate the C-fibers in the trigone thought to be responsible for OAB, while preserving the remaining C-fibers, A $\delta$  fibers, and efferent fibers of the bladder to

sense the degree of luminal filling and provide normal contraction of the bladder wall. This approach is supported by prior studies showing that chemo-denervation of the trigone region alone have lower rates of acute urinary retention compared to chemo-denervation of the bladder body while maintaining similar efficacy.<sup>20,21</sup> Although further study will be necessary to prove clinical safety, these findings suggest that the SBD device procedure will result in a tolerable safety profile.

## 5 | CONCLUSIONS

Our results suggest that the Selective Bladder Denervation device can provide a targeted denervation of the trigone with an appropriate healing response. This may be a promising option for treatment of patients with the Overactive Bladder Syndrome and further clinical studies are warranted.

## ACKNOWLEDGMENTS

Amphora Medical, Inc. is a client of the West Virginia University Pathology Laboratory for Translational Medicine (PLTM). James Coad is the Director of the PLTM, which received funding for the performance of this study; Dr. Coad has no personal financial disclosures. Lynette Phillips and Emily Tobin are employed by American Preclinical Services, which received funding for this study. Eric Whitbrook is the Principle Research and Development Engineer for Amphora Medical, Inc. James Fugett, II, Haydon Bennett, and Joshua ShROUT are employees of the PLTM without personal financial disclosures. The authors acknowledge Amphora Medical, Inc. (Maple Grove, MN) for their financial support of this study and supplying the SBD device.

Funding information

Amphora Medical, Inc.

## REFERENCES

1. Stewart W, Van Rooyen J, Cundiff G, et al. Prevalence and burden of overactive bladder in the United States. *World J Urol.* 2003; 20:327–336. [PubMed: 12811491]
2. Abrams P, Cardozo L, Fall M, et al. The standardisation of terminology of lower urinary tract function: report from the Standardisation Sub-committee of the International Continence Society. *Am J Obstet Gynecol.* 2002;187:116–126. [PubMed: 12114899]
3. Fowler CJ, Griffiths D, De Groat WC. The neural control of micturition. *Nat Rev Neurosci.* 2008;9:453–466. [PubMed: 18490916]
4. de Groat WC. The urothelium in overactive bladder: passive bystander or active participant? *Urology.* 2004;64:7–11. [PubMed: 15621221]
5. Gillespie JI. The autonomous bladder: a view of the origin of bladder overactivity and sensory urge. *BJU Int.* 2004;93: 478–483. [PubMed: 15008713]
6. Andersson KE. Bladder activation: afferent mechanisms. *Urology.* 2002;59:43–50. [PubMed: 12007522]
7. Lee SR, Kim HJ, Kim A, Kim JH. Overactive bladder is not only overactive but also hypersensitive. *Urology.* 2010;75:1053–1059. [PubMed: 20092879]
8. Moulton BC, Fryer AD. Muscarinic receptor antagonists, from folklore to pharmacology; finding drugs that actually work in asthma and COPD. *Br J Pharmacol.* 2011;163:44–52. [PubMed: 21198547]
9. Abrams P, Andersson KE. Muscarinic receptor antagonists for overactive bladder. *BJU Int.* 2007;100:987–1006. [PubMed: 17922784]
10. Bragg R, Hebel D, Vouri SM, Pitlick JM. Mirabegron: a Beta-3 agonist for overactive bladder. *Consult Pharm.* 2014;29: 823–837. [PubMed: 25521658]

11. Sahai A, Dowson C, Khan MS, Dasgupta P. GKT Botulinum Study Group. Repeated injections of botulinum toxin-A for idiopathic detrusor overactivity. *Urology*. 2010;75:552–558. [PubMed: 20035984]
12. Cespedes RD, Cross CA, McGuire EJ. Modified Ingelman-Sundberg bladder denervation procedure for intractable urge incontinence. *J Urol*. 1996;156:1744–1747. [PubMed: 8863585]
13. Westney OL, Lee JT, McGuire EJ, Palmer JL, Cespedes RD, Amundsen CL. Long-term results of Ingelman-Sundberg denervation procedure for urge incontinence refractory to medical therapy. *J Urol*. 2002;168:1044–1047. [PubMed: 12187219]
14. Andersson KE. Bladder activation: afferent mechanisms. *Urology*. 2002;59:43–50. [PubMed: 12007522]
15. Moore KH, Gilpin SA, Dixon JS, Richmond DH, Sutherst JR. Increase in presumptive sensory nerves of the urinary bladder in idiopathic detrusor instability. *BJU Int*. 1992;70:370–372.
16. Simões M, de Souza DB, Gallo C, Pereira-Sampaio MA, Costa WS, Sampaio FJ. Histomorphometric comparison of the human, swine, and ovine collecting systems. *The Anat Rec*. 2016;299:967–972.
17. Yang JM, Huang WC. Bladder wall thickness on ultrasonographic cystourethrography. *J Ultrasound Med*. 2003;22:777–782. [PubMed: 12901404]
18. Üçer O, Gümü B, Albaz AC, Pekindil G. Assessment of bladder wall thickness in women with overactive bladder. *Turk J Urol*. 2016;42:97–100. [PubMed: 27274895]
19. Panayi DC, Digesu GA, Tekkis P, Fernando R, Khullar V. Ultrasound measurement of vaginal wall thickness: a novel and reliable technique. *Int Urogynecol J*. 2010;21:1265–1270. [PubMed: 20502876]
20. Kuo HC. Comparison of effectiveness of detrusor, suburothelial and bladder base injections of botulinum toxin a for idiopathic detrusor overactivity. *J Urol*. 2007;178:1359–1363. [PubMed: 17706718]
21. Kuo HC. Bladder base/trigone injection is safe and as effective as bladder body injection of onabotulinumtoxinA for idiopathic detrusor overactivity refractory to antimuscarinics. *Neurourol Urodyn*. 201:1242–1248.

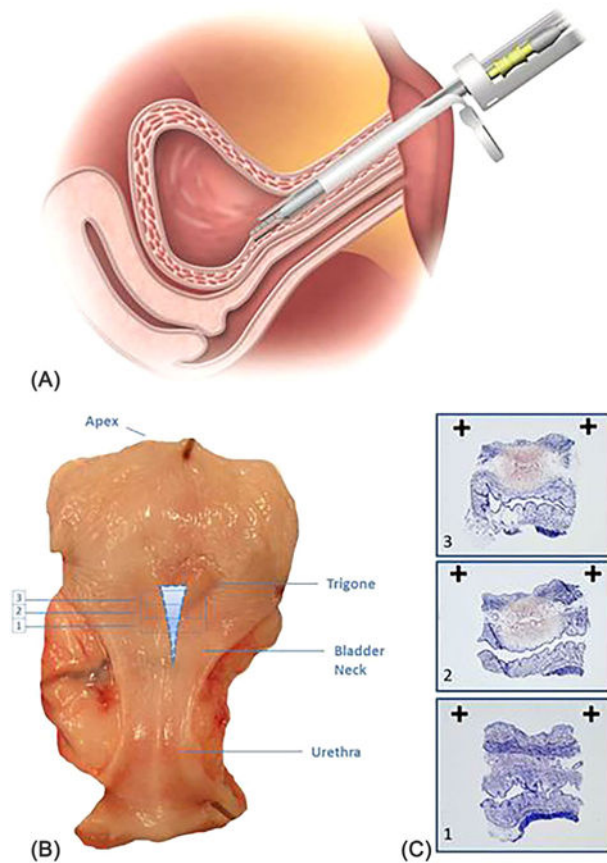


**FIGURE 1.**

A, Illustration of SBD device placement at the bladder trigone. B, Extirpated bladders were ventrally opened from bladder neck to the apex. C, NBT-stained transverse trigone cross sections (from shaded blue triangle correlating with sections 1, 2, and 3) showing the underlying tan NBT-negative ablation (approximately 5 $\times$  magnification and with 2 mm cross bar scale)

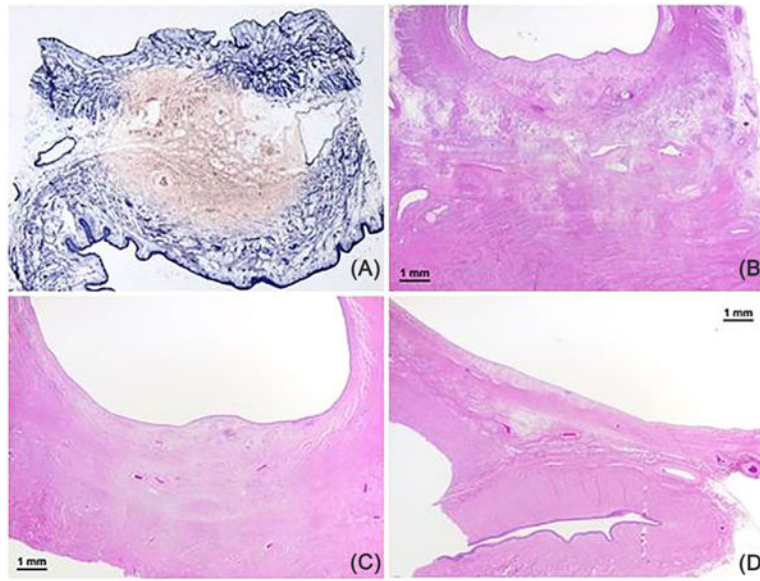


**FIGURE 2.**

Trigone ablation histology. A, Representative NBT staining of a fresh extirpated Day 0 trigone. B, Representative Day 7 trigone ablation (10× magnification, hematoxylin and eosin-stained). C, Representative Day 30 trigone ablation (10× magnification, hematoxylin and eosin-stained). D, Representative Day 90 trigone ablation (10× magnification, hematoxylin and eosin-stained)

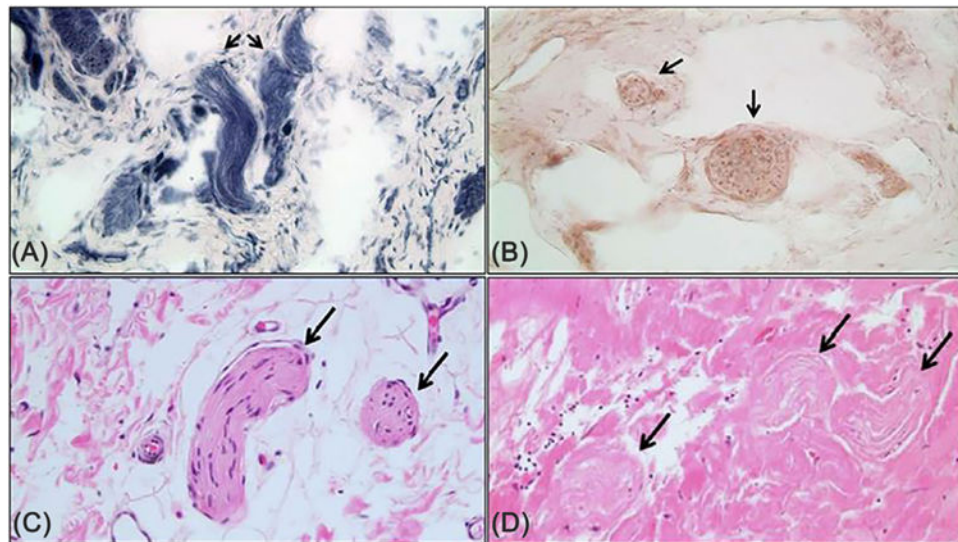


**FIGURE 3.**

Selective bladder denervation following ablation with the SBD Device. Representative NBT viability stained fresh extirpated bladder (Day 0, A and B) and Day 7 post-ablation hematoxylin and eosinstained (C and D) trigone region nerves (100× magnification). A, Viable NBT-positive (purple) nerves are illustrated from the adventitia outside of the ablation (black arrows). B, Non-viable NBT-negative (tan) nerves are illustrated from within the ablation (black arrows). C, Corresponding viable nerves, stained with hematoxylin and eosin, are illustrated from the tissue surrounding the ablation (black arrows). D, Corresponding non-viable necrotic nerves, stained with hematoxylin and eosin, are illustrated from within the ablation (black arrows)

**TABLE 1**  
Ablation associated histology scaled scoring systems for evaluating healing responses

Score	Acute inflammation	Chronic inflammation	Granulation tissue	Fibrosis
0 (None)	Absence of PMNs	Absence of chronic inflammatory cells	Absence of granulation tissue	Absence of collagen fibrosis ( <i>collagen similar to native tissue density</i> )
1 (Minimal)	Rare individual PMNs	Occasional scattered chronic inflammatory cells	Granulation tissue involving less than 10% of the area surrounding ablation	Collagen has a slightly increased fiber density but maintains a fibrillary ( <i>basket weave-like</i> ) architecture
2 (Mild)	Scattered PMNs without clustering	Frequent scattered or focally clustered chronic inflammatory cells	Granulation tissue involving 10-25% of the area surrounding ablation	Collagen fibers are slightly more courser and/or compact ( <i>linearized</i> )
3 (Moderate)	PMNs with focal clustering	Multifocal chronic inflammatory cell clusters	Granulation tissue involving 26-50% of the area surrounding ablation	Collagen fibers are moderately courser and/or compact ( <i>linearized</i> )
4 (Extensive)	PMNs with more confluent infiltration	More confluent chronic inflammatory cell infiltrate	Granulation tissue involving more than 50% of the area surrounding ablation	Collagen fibers appear densely compacted or paucicellular and hyalinized ( <i>hypertrophic scar-like</i> )

TABLE 2

## In vivo ablation associated histologic characteristics

	Mean ± Std Dev	Median	Minimum	Maximum
Day 7 histology				
Ablation width	16.3 ± 1.22 mm	16.3 mm	14.7 mm	17.8 mm
Ablation height	8.4 ± 1.56 mm	8.5 mm	6.5 mm	10.2 mm
Acute inflammation score	0.8 ± 0.8	0.5	0	2
Chronic inflammation score	0.5 ± 0.5	0.5	0	1
Granulation tissue score	1.3 ± 0.4	1.0	1	2
Fibrosis score	0.0 ± 0.0	0.0	0	0
Overall healing stage	Early loose			
Day 30 histology				
Ablation width	13.9 ± 2.84 mm	14.0 mm	10.5 mm	17.3 mm
Ablation height	2.6 ± 0.88 mm	2.3 mm	1.9 mm	4.1 mm
Acute inflammation score	0.8 ± 1.3	0.0	0	3
Chronic inflammation score	2.0 ± 1.0	2.0	1	3
Granulation tissue score	1.0 ± 0.7	1.0	0	2
Fibrosis score	1.8 ± 0.4	2.0	1	2
Overall healing stage	Primary healing			
Day 90 histology				
Ablation width	13.1 ± 4.48 mm	13.1	6.7 mm	19.3 mm
Ablation height	1.3 ± 0.32 mm	1.3 mm	0.9 mm	1.7 mm
Acute inflammation score	0.0 ± 0.0	0.0	0	0
Chronic inflammation score	2.3 ± 1.1	2.0	1	4
Granulation tissue score	0.0 ± 0.0	0.0	0	0
Fibrosis score	3.0 ± 0.0	3.0	3	3
Overall healing stage	Secondary healed			